

# 1 Sand throwing in a pit-building antlion larva from a soil mechanical 2 perspective

3  
4 Sebastian Büsse<sup>1\*</sup>, Thies H. Büscher<sup>1</sup>, Lars Heepe<sup>1</sup>, Stanislav N. Gorb<sup>1</sup> & Hans Henning  
5 Stutz<sup>2</sup>

6  
7 <sup>1</sup> Functional Morphology and Biomechanics, Institute of Zoology, Kiel University, Kiel,  
8 Germany

9 <sup>2</sup> Department of Engineering, Geotechnical Engineering, Aarhus University, Aarhus,  
10 Denmark

11  
12 \*Corresponding author: [sbuesse@zoologie.uni-kiel.de](mailto:sbuesse@zoologie.uni-kiel.de)

## 13 14 **Abstract**

15 Sandy pitfall traps are an elaborate construction to capture prey and antlions are well-known  
16 representatives of this predation technique. From a soil mechanical perspective, antlions  
17 exploit the interactions between the particles of their habitat and engineer a stable trap. This  
18 construction is close to the unstable state, where a prey item will immediately slide towards  
19 the center - towards the ambushing antlion - when accidentally entering the trap. This method  
20 is efficient, but requires permanent pit maintaining. According to the present knowledge,  
21 antlions throw sand at their prey, to distract it, and/or cause sand slides towards the center of  
22 the pit. Using sand throwing and escape experiments, as well as finite element analysis, we  
23 supported this hypothesis. Furthermore, we added new hypothesis about maintaining the  
24 pitfall trap. We showed that sand that accumulates in the center of the pit will be continuously  
25 removed, which lead to the slope maintenance close to an unstable condition. This avoids  
26 self-burial of the antlion, as well as decreasing the chance of prey item escapes by keeping  
27 the slope angle steep. This demonstrates the interaction of an insect larva with its abiotic  
28 environment from a novel perspective and adds further insights into longstanding  
29 entomological hypotheses.

30  
31 **Keywords:** *Euroleon nostras*, self-stratification, soil mechanics, finite element modelling,  
32 prey capturing, predatory strike, trap-building predators, angle of repose

## 33 34 **Background**

35 Trap-building is a highly specialised, but comparably uncommon, hunting strategy within the  
36 animal kingdom (Franks et al. 2019). Most trap-building invertebrates employ silk in their  
37 constructions, with orb-web spiders probably being the most prominent example (Denny

38 1976; Vollrath and Knight 2001). These invertebrates successfully use silk to capture prey  
39 (Lin et al. 1995; Krink and Vollrath 2000; Venner et al. 2006). In contrast, the construction of  
40 traps without the employment of silk is best known in wormlions (Diptera: Vermileonidae) and  
41 antlions (Neuroptera: Myrmeleontidae), using sand to dig a pitfall trap (Fig. 1 B,C) (cf. Adar et  
42 al. 2016) with a few exceptions (cf. Dejean et al. 2005). Even though the trap-digging  
43 strategy in antlions (spiral digging) is considered more effective in comparison to central  
44 digging in wormlions (Tuculescu 1975; Franks et al. 2019), pitfall trap building strategies of  
45 worm- and antlions represent an excellent example for convergent evolution of behaviour  
46 (Miler et al. 2018).

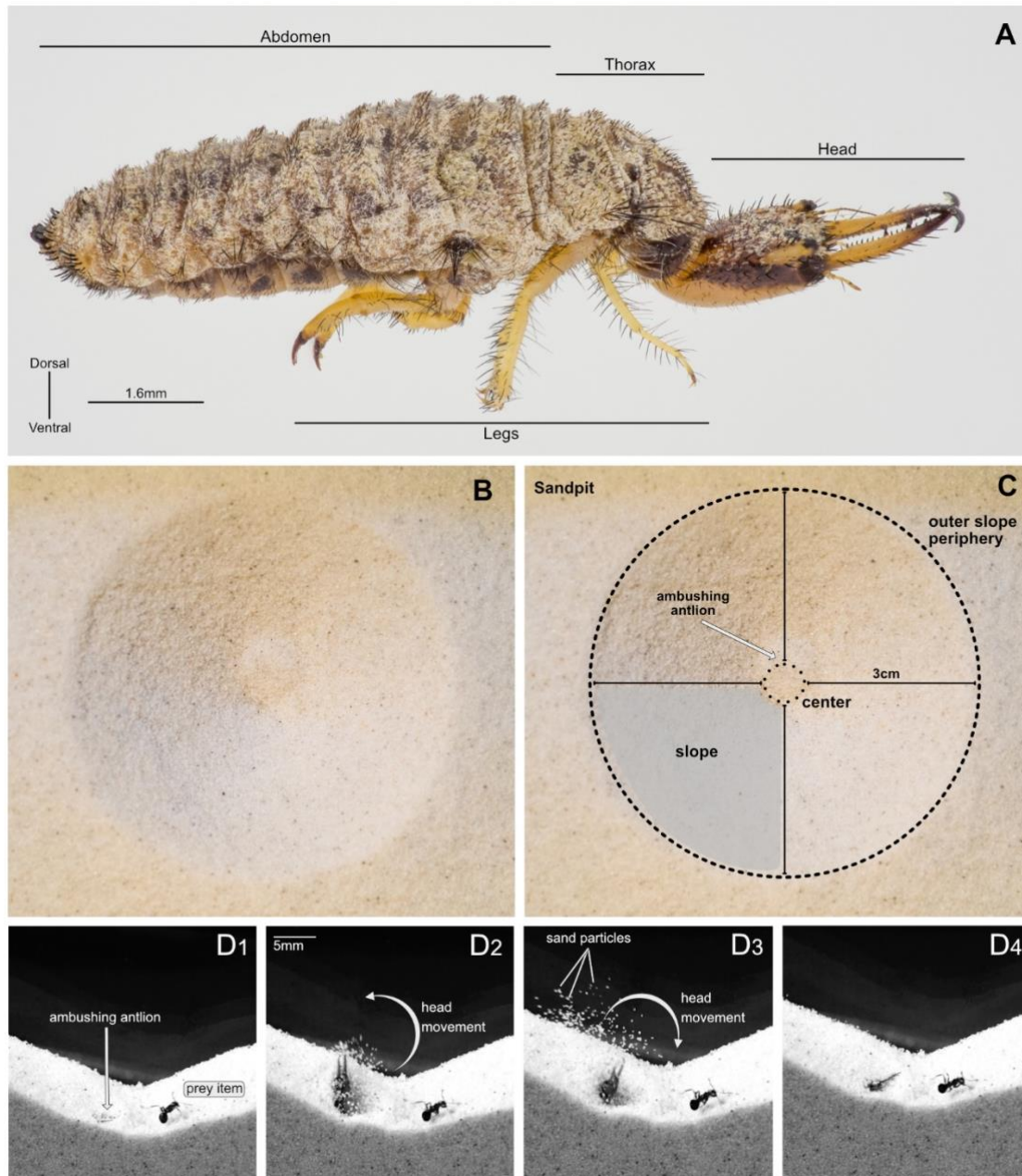
47  
48 Generally, ground-dwelling animals which inhabit sandy habitats are strongly affected by the  
49 physical characteristics of the substrate. Sand is a collection of particles interacting with each  
50 other via contact forces. Here, spontaneous organisation (Rosato et al. 1987; Möbius et al.  
51 2001) faces natural stratification (Bak et al. 1987; 1988), which leads to an irregular solid-  
52 pore system (Herrmann 1998). Whereas the number of pores in granular media influences  
53 the stress-deformation behaviour to a great extent, loose packing of granular particles leads  
54 to an instable construct that can easily reach an unstable state (Terzaghi 1943, Miura et al.  
55 1997). Here more voluminous sand grains show a larger angle of repose (definition see  
56 "Methods: Terminology") than less voluminous grains, and all interact with the successive  
57 sand layers (Makse et al. 1997).

58  
59 The juvenile stages of most antlion species (Myrmeleontidae) utilise exactly this soil  
60 mechanics phenomenon. The laval antlion (Fig.1 A) is a pit-building ambush predator  
61 (Franks et al. 2019). The hunting success of it largely depends on the abiotic factors of its  
62 habitat (Scharf and Ovadia 2006; Bar-Ziv et al. 2019), such as sand grain size and  
63 distribution, and the majority of antlion species prefer sand with a comparably small particle  
64 size (Allen and Croft 1985; Loiterton and Magrath 1996; Botz et al. 2003; Farji-Brener 2003).  
65 Suitable substrates will enable the construction of considerably larger pits (Barkae et al.  
66 2012), resulting in the ability to capture larger prey and reducing the risk of prey escapes  
67 (Griffiths 1980; Lucas 1982; Heinrich and Heinrich 1984; Scharf et al. 2018). The relationship  
68 between sand properties and slope is the key difficulty for prey items captured in a sandy  
69 pitfall trap, as shown for the ant species *Aphaenogaster subterranea* (Latreille, 1798). This  
70 species copes with the unstable substrate with a gait pattern transition from the tripod gait to  
71 the metachronal wave pattern (Humeau et al. 2019). Changing the gait to the one involving a  
72 higher number of legs (e.g. metachronal wave) is known from other insects adapting to  
73 challenging attachment conditions (e.g. walking on the ceiling), and thus risking to lose their  
74 grip to the substrate (Gorb and Heepe 2017; Büscher and Gorb 2019). Thus, the pitfall trap

75 of an antlion is a mechanically unstable construction, and its capturing success is increasing  
76 with increasing slope angles and positively affected by decreasing sand particle size (Botz et  
77 al. 2003). Exploiting the instability of the slope, the trap's morphology (Fig. 1 B,C) is used to  
78 facilitate hunting prey of very different kind and size (cf. Gepp and Hölzel 1989). The larval  
79 antlion is ambushing in the vertex of the pit (Lambert et al. 2011), where it is throwing sand,  
80 using fast flicks of its head (Fig. 1 D<sub>1</sub>-D<sub>4</sub>; Griffiths 1980; Gepp and Hölzel 1989; Lambert et  
81 al. 2011). This behaviour intends the distraction of escaping prey and more importantly,  
82 causes small sand slides to trap the prey and translocate it to the center of the vertex –  
83 respectively towards the antlion (Griffiths 1980).

84

85 We here present a study of the soil mechanical behavior that ensure the antlion's prey  
86 capturing success. Underlining the sandslide theory, mentioned above, on the one hand, we  
87 present a supplementary hypothesis focusing on pit maintaining, on the other. Presumably,  
88 the sand throwing will not only actively prevent the prey from escaping, but will also maintain  
89 the required instability of the slope. The sand, which will accumulate at the center of the pit  
90 by the movements of the escaping prey, will be removed and more importantly the slope will  
91 be kept close to an unstable condition. This study exemplifies the benefits of an  
92 interdisciplinary approach to evaluate a known phenomenon from the perspective of two  
93 different scientific disciplines aiding in the understanding of the underlining mechanisms –  
94 here of the sand throwing by antlion larvae.



95

96

97 Figure 1: Antlion and pitfall trap. A. Habitus of antlion larva (*Eurolion nostras*), lateral view. B-C.

98 Sandpit used from the antlion as pitfall trap. C. Same sandpit as in B including labels. D. Sand

99 throwing behaviour of the antlion by the flick of its head. D1-4. Time series based on single frames

100 obtained from high-speed videography: 1. Before the flick of the antlion head starts; 2. During the flick,

101 upwards movement of the antlions head; 3. During the flick, downward movement of the antlions

102 head; 4. After the flick of the antlion head.

103

## 104 **Methods**

105

### 106 *Terminology*

107 **Angle of repose:** Physically, the angle of repose is described as the angle at which a  
108 transition between phases of granular materials happening. The adopted common definition  
109 is the steepest slope angle of the unconfined granular material measure from the horizontal  
110 axis.

111  
112 **Friction angle:** The friction angle defines the frictional shear resistant of the soil dependent  
113 of the normal effective stress.

114  
115 **Cohesion:** The cohesion is the shear strength component of the soil that is independent of  
116 the inter-particle friction.

117  
118 **Mobilised friction:** This is the definition of the friction that was mobilised in the strength  
119 reduction method using the finite element model.

120

#### 121 *Sand throwing experiments*

122 Larvae of *Euroleon nostras* (Fourcroy, 1785) were kept in small ant-terrariums  
123 (210x100x105mm) filled with sand (particle size: 125  $\mu\text{m}$ ). Prior the experiments, the antlion  
124 had 24h for setting up their pitfall trap. We used small instars of the house cricket (*Acheta*  
125 *domesticus* (Linnaeus,1758)) as well as black garden ants (*Lasius niger* (Linnaeus,1758) and  
126 *L. fuliginosus* (Latreille, 1798)) to film the prey capturing process of the antlion larvae using  
127 an Olympus OMD 10mkII digital camera (Olympus K.K., Tokyo, Japan) equipped with a  
128 Leica 45mm macro lens (Leica, Wetzlar, Germany). For measuring the slope angles (N=9,  
129 total sequences 16) and for further image processing, Affinity Photo and Affinity Designer  
130 (Serif Ltd, Nottingham, United Kingdom) were used. The slopes before and after sand  
131 throwing were compared via a paired t-test, as the data was normally distributed (according  
132 to Shapiro-Wilk's test for normality, P=0.08), using SigmaPlot 12.0 (Systat Software Inc., San  
133 José, CA, USA).

134

#### 135 *Escape experiments*

136 For the escape experiments a small formicarium (210x100x105mm) was used to film house  
137 crickets (*A. domesticus*) while trying to escape a conical half-shaped artificial pitfall trap. The  
138 formicarium was filled with sand (particle size: 125 $\mu\text{m}$ ) using a defined funnel to produce a pit  
139 close to the unstable state. Furthermore, we used ants (*L. niger* and *L. fuliginosus*) to escape  
140 from a conical artificial pitfall trap. To produce this pit a box was filled with sand (see above)  
141 with a hole in the bottom to produce a pit close to the unstable state. The prey items were  
142 filmed, using an Olympus OMD 10mkII digital camera (Olympus K.K., Tokyo, Japan)  
143 equipped with a Leica 45mm macro lens (Leica, Wetzlar, Germany), while ascending the

144 slope of the pit (N=7). Furthermore, a house cricked was filmed, using a Go-Pro Hero 5  
145 (GoPro Inc., San Mateo, US) in time lapse setting (1 frame/min), over the course of 12h by  
146 trying to escape the pit (respectively the terrarium), without the maintaining of an antlion. For  
147 measuring the slope angles and for further image processing, Affinity Photo and Affinity  
148 Designer (Serif Ltd, Nottingham, United Kingdom) were used.

149

### 150 *Photography*

151 For stacked photography, we used a custom-made 3D-printed LED illumination dome system  
152 (Bäumler et al. 2020) and an Olympus OMD 10mkII digital camera (Olympus K.K., Tokyo,  
153 Japan), equipped with a Leica 45mm macro lens (Leica Camera AG, Wetzlar, Germany).  
154 In general, all images were subsequently processed in Affinity Photo and Affinity Designer  
155 (Serif Ltd, Nottingham, United Kingdom).

156

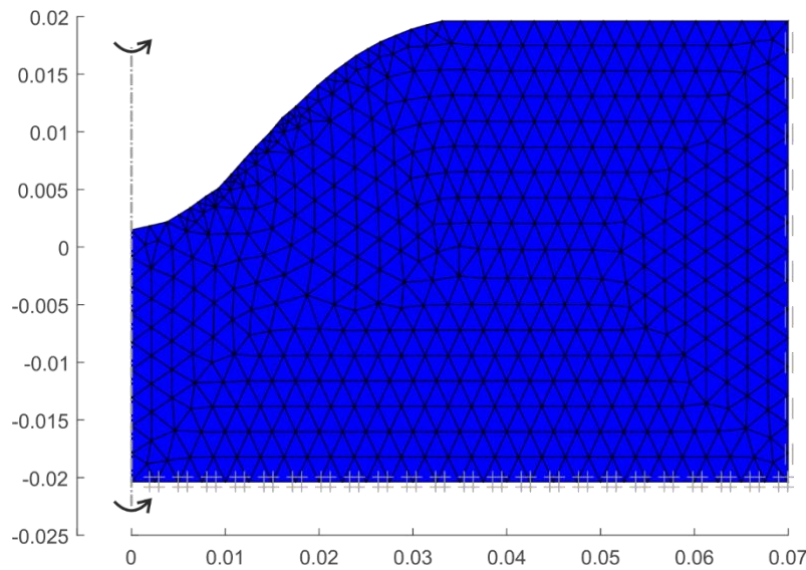
### 157 *Finite-element simulations*

158 The simulations are conducted using the finite-element method (FEM; commercial software  
159 package OPTUM G2 2020, Copenhagen, Denmark). For studying the slope stability, the  
160 strength reduction method has been applied to simulate the progressive failure of the sand  
161 slope that is built by the antlion larvae as pitfall trap. The underlying principle of the strength  
162 reduction method is that the initially assigned soil strength parameters will be reduced until a  
163 failure occurs in the soil continuum. A detailed description of the strength reduction method is  
164 given in e.g. Tschuchnigg et al. (2015a; 2015b). In short, the strength reduction method is  
165 used to estimate the stability of a soil mechanical system by reducing systematically the  
166 strength parameters of soil, namely cohesion and the friction angle. For the assessment of  
167 the failure, the factor of safety (FoS) is used as:

$$168 \quad FoS = \frac{\tan \varphi'}{\text{mobilised } \tan \varphi'} = \frac{c'}{\text{mobilised } c'}$$

169 Where  $\tan \varphi'$  is the effective friction angle of the soil and  $c'$  is the effective cohesion of the  
170 soil. Herein, the friction angle and the cohesion describe the shear strength of a soil using  
171 the concept of the Mohr-Coulomb failure criterion (Mohr 1900). The friction angle defines the  
172 friction shear resistant of the soil dependent of the normal effective stress. The cohesion is  
173 the shear strength component of the soil that is independent of the interparticle friction.  
174 These are divided by mobilised friction and cohesion. The mobilised friction  $\tan \varphi'$  and  
175 cohesion describe the values that could be applied in the strength reduction method.  $FoS < 1$   
176 describe a failure and  $FoS > 1$  describe a stable pit slope. The axisymmetric geometry of the  
177 initial reference pit is shown in Figure 2. The boundary conditions at the bottom of the model  
178 are fixed for all degree of freedoms, and the right side is a slider boundary condition.

179



180

181 Figure 2: Axi-symmetric mesh for the initial slope model, using 1000 (15-noded) elements. The soil  
182 (blue) is modelled using the linear elastic – perfectly plastic Mohr-Coulomb model.

183

184 The model used in the simulations is the linear elastic-perfectly plastic Mohr-Coulomb  
185 constitutive model, which have been proven to be sufficient for such ultimate limit state  
186 simulations (Davis 1968, Tchuchnigg et al. 2015). The used geometry is chosen based on  
187 the previously reported average antlion pits (e.g. Bongers & Koch 1981; Lucas 1982) and our  
188 experimental setup.

189

190 In general, the following steps are conducted for each simulation:

- 191 1). The initial stress is applied and calculated.
- 192 2.) The initial geometry is analysed to estimate the initial FoS.
- 193 3.) The changed geometry is used to estimate the change in the FoS and the consequences  
194 due to the sand throwing of the antlion larvae.

195

196 The reference configuration (Fig. 2) has an initial FoS= 1.096, and this means the slope  
197 geometry is stable. For the more accurate prediction of the failure mechanisms and the FoS,  
198 a mesh adaptivity step is applied with three adaptive iterations using the shear dissipation as  
199 adaptivity control. The mesh adaptivity is a procedure using an adaptive meshing technique  
200 to refine the mesh around the shear zone in which the plastic deformation is overdriven (Ortiz  
201 & Quigley 1991). The mesh is refined according to the norm of the strain vector  $\|\epsilon\|$ . The  
202 initial model shown in figure 2, shows a mesh consisting of 1000 elements; here, the model  
203 is using a linear elastic – perfectly plasticity Mohr-Coulomb constitutive model (Mohr 1900).  
204 The parameters used in the simulation are given in Table 1. In the mesh refinement step,  
205 2000 elements are used.

206 Table 1: Parameters used in the finite-element simulations for the Mohr-Coulomb model (grey zones  
207 do not influence the strength reduction method)

Material	Cohesion c [kPa]	Friction angle $\varphi$ [°]	Dilatancy [°]	E-modulus [MPa]	Poisson's ratio [-]
Sand initial	0	34.5	0	20	0.2
Sand reduced density	0	29	0	20	0.2

208  
209 In total, six different simulations were conducted. In these simulations, the slope geometry  
210 was changed to simulate the throwing behaviour of the antlion larvae (Case 1 & 2). In two  
211 simulations, the soil was simulated with reduced friction angle zones (Case 3 & 4), based on  
212 the looser soil state. This looser state is based on the assumption of generation of looser soil  
213 zones due to the sand throwing behavior. This was done to screen the effect, when there is  
214 no volume loss in the sand. In the last two simulations, the change in geometry (sand  
215 throwing) and change in density was applied (Case 5 & 6). Based on the sand throwing  
216 experiments and the experimental observations. The modelling assumption here is that a  
217 looser granular packing has a smaller angle of friction (Mitchell & Soga 2005). The changes  
218 in the geometry and the changes in the areas with smaller friction angles are indicated in  
219 Table 2.

220  
221 Table 2: Change in model areas to simulate the six different case via strength reduction method

Case	Area of slope geometry change [mm <sup>2</sup> ]	Area of change in friction angle [mm <sup>2</sup> ]
1	4.64	-
2	3.40	-
3	-	15.66
4	-	8.19
5	4.64	12.13
6	3.40	11.48

222  
223 This selection aims to model the different effects induced on the soil by the antlions sand  
224 throwing behaviour, to study the effect of the antlion trap/pit slope stability. The figures were  
225 prepared with MATLAB (R2019b, The Mathworks Inc., Natick Massachusetts) using the data  
226 files form OptumG2.

227  
228 All experiments and simulations were conducted considering a dry sand character, the effect  
229 of partially saturation of the soil was not studied.

230



## 231 Results

232 We used the insights from biological experiments considering the soil mechanical properties  
233 of the antlions' trap building and combined these with finite element simulations to identify  
234 the underlying soil mechanical behaviour.

235

### 236 *Sand throwing experiments*

237 After allowing the antlion larvae to set up a pitfall trap for 24h, all formicariums for the  
238 experiment exhibited a sandpit ready to capture prey. After inserting a prey item into the  
239 terrarium, the antlions start throwing sand (Fig. 1, supplemental videos 1-3), when noticing  
240 the vibrations of the prey. The sand throwing can start without visible sand movement, but  
241 becomes more frequent (sand throwing and therefore sand movement), when the prey item  
242 changes the slope geometry and especially when moving sand from the slope towards the  
243 center of the pit (respectively towards the ambushing antlion). The sand throwing of the  
244 antlion usually causes small sand slides (supplemental video 1) distracting the prey and/or  
245 causing the prey sliding towards the center of the pit (supplemental video 2). However, it  
246 becomes obvious that these sand slides also recover the steepness of the sandpit's slope -  
247 smoothed by the movement of the prey or the antlion itself (Fig. 3, supplemental video 3).  
248 The average slope angle before sand throwing of the antlion is  $27.3 \pm 2.7^\circ$  (min.  $22.5^\circ$ ,  
249 max.  $31.5^\circ$ ), the average slope angle after sand throwing of the antlion is  $31.1 \pm 2.1^\circ$   
250 (min.  $26.5^\circ$ , max.  $34.5^\circ$ ) resulting in an average slope angle change of  $3.44^\circ$  (min.  $-1^\circ$ , max.  
251  $7^\circ$ ). The sand throwing of the antlion results in a significantly steeper slope after the action  
252 (paired t-test,  $t=-8.095$ , d.f.=8,  $N_{1,2}=9$ ,  $P \leq 0.001$ ).

253



254

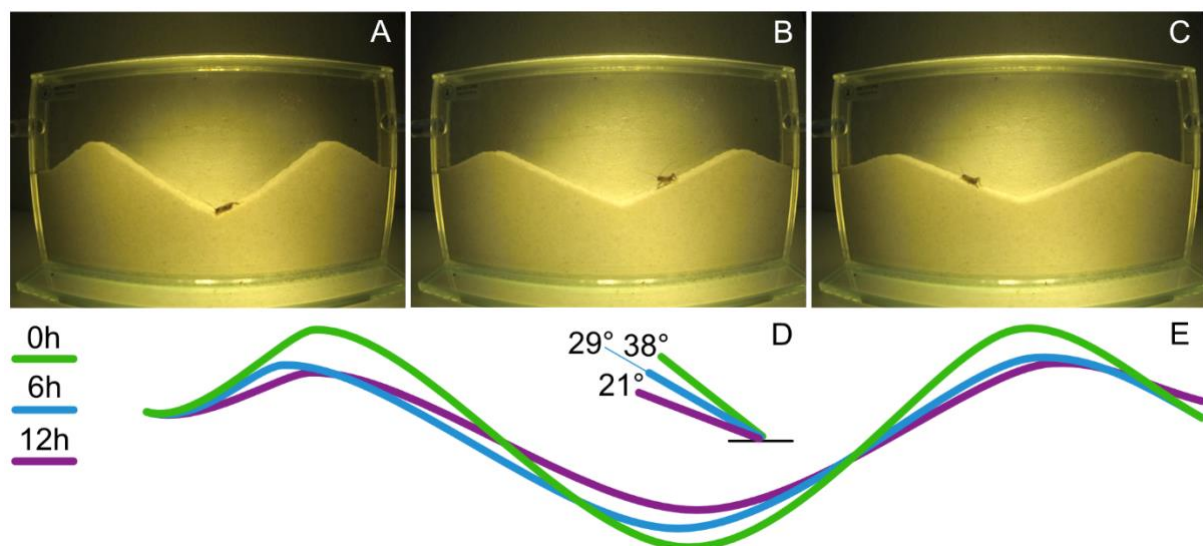
255

256 Figure 3: Slope of a sandpit before and after sand throwing by the antlion. A. Already leveled slope  
257 (caused by the prey item, house cricket on the left side) before the sand throwing of the antlion. Red  
258 line indicates the slope angle of 25.5°, the grey line indicates the reference angle. B. Slope after the  
259 sand throwing of the antlion. Blue line indicates the new slope angle of 31°, red line of the old slope  
260 angle in transparent, the grey line indicates the reference angle. C. Box-whisker-plots of initial (before)  
261 and resulting (after) slope angles of the pit. The line represents the median, the box and whiskers the  
262 10, 25, 75 and 90 % percentiles, respectively. \*  $P \leq 0.001$ , paired t-test.

263

### 264 *Escape experiments*

265 The restructuring of the sand topography within the artificial sandpits reveals the influence of  
266 the distortion, a prey item causes without the influence of maintaining the pit by the antlion  
267 (Fig. 4, supplemental video 4 and 5). The escape efforts of the prey item can cause serious  
268 damage to the sandpit geometry, especially to the slope angle. The slope in the 12h  
269 experiment decreases from 38° over 29° after 6h, to 21° after 12h (Fig. 4, supplemental  
270 video 4). However, even single events (one walk of a cricket or ant on the slope) can cause  
271 sand movements and therefore changes in the overall slope geometry. Sand is pushed  
272 downwards, towards the center of the slope by every step of the prey item. Every step is,  
273 therefore, changing the slope geometry slightly, as well as pushes small volumes of sand to  
274 the center of the pit. The influence of several steps of the prey item accumulates over time.  
275 Consequently, with an increasing dwelling time of the prey in the pit, the change of the  
276 sandpit geometry leads to an increasing chance of its escape (supplemental video 5).  
277



278  
279 Figure 4: Escape experiment: house cricket over the course of 12h in a formicarium. A-C. Change of  
280 the artificial pit geometry over the course of 12h. A 0h. B 6h. C 12h. D. Change of the slope angle over  
281 the course of 12h, green line after 0h, blue line after 6h and violet line after 12h. E. Change of the  
282 artificial sandpit geometry over the course of 12h shown as schematic, green after 0h, blue after 6h  
283 and purple after 12h.

284

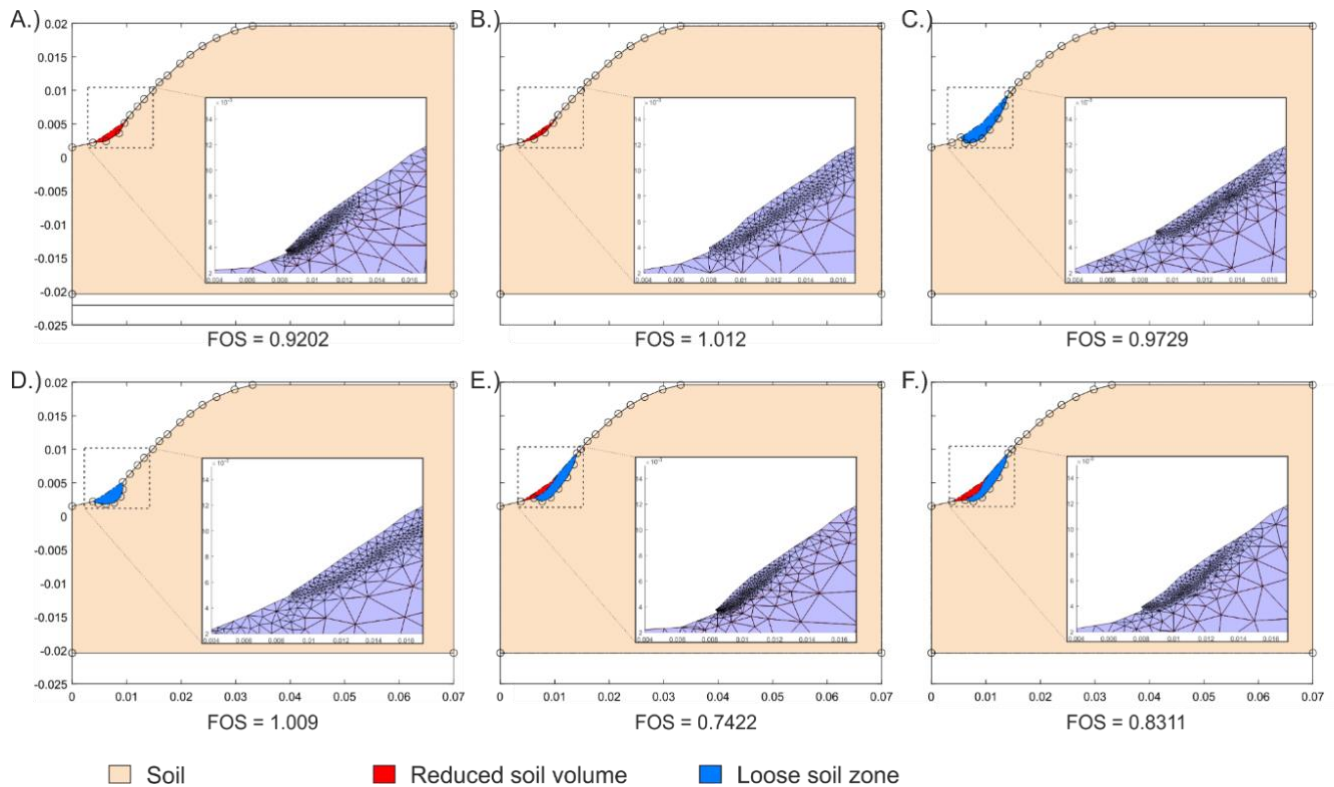
### 285 *Finite-element analysis*

286 The results of the conducted finite element analysis are shown in Figure 5. The first two initial  
287 cases (case 1 and 2; Fig. 5 A,B, see also Table 2) demonstrate the effect of a factor of safety  
288 (FoS) reduction, based on a slight change in the slope geometry. Depending on this  
289 geometry change (case 2, Figure 5 B), the FoS can result in a value below 1.0, which  
290 indicate an unstable slope (initial slope geometry FoS = 1.096). This change in the slope  
291 angle could be observed in the sand throwing experiments (see Figure 3 A, B). Herein, a

292 local change of the slope geometry can generate an unstable slope. In figure 5 (C,D), the  
293 results of the cases 3 and 4 with a pure change in density are simulated without a change in  
294 the slope geometry. Here it can be seen that a change in density may be caused by the  
295 movement and throwing behavior of the ambushing antlion and can lead to an unstable  
296 condition.

297 Generally, local changes do not necessarily lead to an unstable situation (see Fig. 5 D; FoS,  
298 1.009). Whereas, a combination (cases 5 and 6) of a change in the slope geometry (case 1  
299 and 2; Fig. 5 A,B) with a change in density of the soil (represented by a change in the friction  
300 angle; case 3 and 4) leads to an unstable condition. Cases 5 and 6 (Fig. 5 E,F) are the most  
301 realistic natural scenarios compared to the described sand throwing experiments. In both  
302 cases, the FoS is below 1.0, which indicates an unstable slope.

303



305 Figure 5: Results for the Cases 1 – 6 (A.-F.) with the indicated change of the reduced soil volume (in  
306 red), the changed zones for the friction angle (in blue) and the results, shown as failure surfaces with  
307 different adaptive meshes, which demonstrate the failure mechanisms.

308

309 Besides an adaptive remeshing was used to refine the mesh around plastic zones in the soil.  
310 The use of the remeshing technique lead to small element sizes close to zones of localized  
311 deformations (shear zones). Therefore, the meshes shown in figure 5 indicate the different  
312 failure geometries and shear zones, which are similar to the geometries in the sand throwing  
313 experiments (Figure 3 and supplementary video material).

314

## 315 **Discussion**

316 The results of the sand throwing and escape experiments are combined with the finite  
317 element simulations to underline the resulting hypothesis as well as add a new soil-  
318 mechanical hypothesis. The sand throwing behaviour of antlion larvae is used during pit  
319 building (Bongers & Koch 1981) as well as prey capturing (Griffiths 1980). During pit building,  
320 the antlion sorts the sand grains towards a preferably smaller grain size (Allen and Croft  
321 1985; Loiterton and Magrath 1996; Botz et al. 2003; Farji-Brener 2003) by the sand throwing,  
322 which allows for larger and more stable pits (Barkae et al. 2012). Further, during prey  
323 capturing, the sand throwing is used to cause small sand slides that displace the prey item  
324 towards the ambushing antlion (Griffiths 1980). However, a prey item can cause significant  
325 structural damage to the pit's geometry (cf. escape experiments). Therefore, pit maintaining  
326 is vital for the antlions prey capturing success. Since antlions usually built their pits close to  
327 the natural equilibrium condition of the slope (Botz et al. 2003) given by the angle of repose  
328 of the granular media (Allen and Croft 1985; Loiterton and Magrath 1996; Botz et al. 2003;  
329 Farji-Brener 2003), the pit's slope is highly unstable and delicate to disturbances (Lucas  
330 1982). Here, without the maintenance by the antlion, the slopes are unstable and the prey  
331 causes an irreversible deformation to the slope angle (slope angle reduction; Fig. 4).  
332 Therefore, without constant maintaining of the pitfall trap (during prey contact), the antlion  
333 befalls self-burial and the slope angle shallows (Fig. 4), so that a prey item can more easily  
334 escape. However, the capturing success is increasing with an increasing slope angle causing  
335 a prey item more likely to slide towards the center of the pit (Botz et al. 2003). As indicated in  
336 the sand throwing experiment, the slope inclination increases by the sand throwing behaviour  
337 of the antlion leading to retaining an unstable state (Fig. 3), the fact highly supporting the pit  
338 maintaining hypothesis.

339

340 From a soil mechanical perspective, the soil state is changing from looser to a denser state  
341 as the thrown sand causes a reorganization of the particles along the slope of the trap. The  
342 sandparticles sliding towards the center of the pit are rearranged during this relocalisation  
343 and come to rest in a denser conformation. The finite element simulation supports our  
344 observations and experiments, because only a combined mechanism (cases 5 and 6,  
345 change in density and sand volume) brings the slope to an unstable state from an initial  
346 stable one (mean slope angle change of  $3.44^\circ$ , Fig. 3), as the factor of safety (FoS) of 0.74  
347 (case 5) and 0.83 (case 6) clearly shows. On the other hand, the finite element simulations  
348 underline the previous hypothesis that the sand throwing causes small sandslides (Griffiths  
349 1980), as also shown in the supplemental videos (1 and 2). Here the change of FoS under 1  
350 (unstable state) in the simulation is indicating that the sand indeed slides towards the center

351 of the pitfall trap. Additionally, sand slides may provide the information to the sensory system  
352 of the predator about an optimal repose angle of the pit.

353

## 354 **Conclusions**

355 We challenged the prevailing hypothesis on antlion sand throwing by investigating the  
356 mechanism with a combination of sand throwing observations, escape experiments as well  
357 as finite element simulations. Our results support the existing hypothesis that small sand  
358 slides displace the prey item towards the ambushing antlion (Griffiths 1980), but furthermore  
359 add a soil mechanical perspective to this behaviour: pitfall traps of antlion larvae are  
360 mechanically unstable constructions, where the prey capturing success increases with an  
361 increasing slope angle. We show that a prey item can considerably change the slope  
362 geometry (flatten the slope) in the course of 12 h (if no antlion is involved; see. Fig. 4).  
363 Furthermore, the sand throwing experiments reveal significantly higher slope angles after the  
364 sand throwing (if a prey item is involved; see Fig. 3). We hypothesize, that sand throwing  
365 functions as the trap maintenance mechanism, to keep the critical slope angle and  
366 counteracts self-burial of the antlion itself.

367

368 **Ethics:** Insect specimens used in this study are not protected, and no ethical statement is  
369 necessary. **Data accessibility:** All raw data will be uploaded to Dryad

370 **Authors' contributions:** SB, LH, SNG and HHS designed the project and developed the  
371 concept of the study. THB and SB reared the antlions. SB and THB performed the high-  
372 speed video recordings and the experiments. SB and THB analysed the biological  
373 experiments and performed the statistics. HHS performed the finite element analysis. HHS  
374 and LH formulated the physical principles and analysed the finite element analysis. SB,  
375 THB, SNG and HHS wrote the manuscript. All authors agree to be held accountable for the  
376 content therein and approve the final version of the manuscript.

377 **Competing interests:** We declare we have no competing interests.

378 **Funding:** SB was directly supported through the DFG grants BU3169/1-1 and BU3169/1-2.

379 **Acknowledgements:** We are grateful for the support of the members of the Functional  
380 Morphology and Biomechanics Group at Kiel University, especially J. Heepe for providing the  
381 samples. We could not accomplish this study without the help of Jonathan Neumann  
382 (University of Potsdam). The discussions with Prof. Dr. Franz Tschuchnigg are highly  
383 appreciated by HHS.

384

## 385 **References**

386

387 Franks NR, Worley A, Falkenberg M, Sendova-Franks AB, Christensen

- 388 K. 2019 Digging the optimum pit: antlions, spirals and spontaneous stratification.  
389 *Proc. R. Soc. B* **286**, 20190365. (doi: 10.1098/rspb.2019.0365)  
390
- 391 Denny MW. (1976) The physical properties of spider's silk and their role in the design of orb-  
392 webs. *J. Exp. Biol.* **65**, 483–506.  
393
- 394 Vollrath F, Knight DP. 2001 Other spinning arthropods (liquid crystalline spinning of spider  
395 silk). *Nature* **410**, 541–548. (doi:10.1038/35069000)  
396
- 397 Lin LH, Edmonds DT, Vollrath F. 1995 Structural engineering of an orb-spider's web. *Nature*  
398 **373**,146–148. (doi:10.1038/373146a0)  
399
- 400 Krink T, Vollrath F. 2000 Optimal area use in orb webs of the spider *Araneus diadematus*.  
401 *Naturwissenschaften* **87**, 90–93. (doi:10.1007/s001140050017)  
402
- 403 Venner S, Chade's I, Bel-Venner MC, Pasquet A, Charpillet F, Leborgne R. 2006 Dynamic  
404 optimisation over infinite-time horizon: webbuilding strategy in an orb-weaving spider as a  
405 case study. *J. Theor. Biol.* **241**, 725–733. (doi:10.1016/j.jtbi.2006.01.008)  
406
- 407 Adar S, Dor R, Scharf I. 2016 Habitat choice and complex decision making in a trap-building  
408 predator. *Behav. Ecol.* **27**, 1491–1498. (doi:10.1093/beheco/arw071)  
409
- 410 Dejean A, Solano PJ, Ayroles J, Corbara B, Orivel J. 2005 Arboreal ants build traps to  
411 capture. *Nature* **434**, 973.  
412
- 413 Tuculescu R, Topoff H, Wolfe S. 1975 Mechanisms of pit construction by antlion larvae. *Ann.*  
414 *Entomol. Soc. Am.* **68**, 719–720. (doi:10.1093/aesa/68.4.719)  
415
- 416 Miler K, Yahya BE, Czarnoleski M. 2018. Different predation efficiencies of trap-building  
417 larvae of sympatric antlions and wormlions from the rainforest of Borneo. *Ecol Entomol* **43**,  
418 255–262.  
419
- 420 Rosato A, Strandburg KJ, Prinz F, Swendsen RH. 1987 Why the Brazil nuts are on top: size  
421 segregation of particulate matter by shaking. *Phys. Rev. Lett.* **58**, 1038–1040.  
422 (doi:10.1103/PhysRevLett.58.1038)  
423

- 424 Möbius ME, Lauderdale BE, Nagel SR, Jaeger HM. 2001 Size separation of granular  
425 particles. *Nature* **414**, 270. (doi:10.1038/nature08115)
- 426 Bak P, Tang C, Wiesenfeld K. 1987 Self-organised criticality: an explanation of the 1/f noise.  
427 *Phys. Rev. Lett.* **59**, 381–384. (doi:10.1103/PhysRevLett.59.381)
- 428
- 429 Bak P, Tang C, Wiesenfeld K. 1988 Self-organised criticality. *Phys. Rev. A* **38**, 364–375.  
430 (doi:10.1103/PhysRevA.38.364)
- 431
- 432 Herrmann HJ. 1998 *On the Shape of a Sandpile*. In: Herrmann HJ, Hovi JP, Luding S  
433 (eds). *Physics of Dry Granular Media*. NATO ASI Series: Applied Sciences. Dordrecht,  
434 Germany: Springer.
- 435
- 436 Terzaghi K. 1943 *Theoretical soil mechanics*. New York, NY: Wiley and Sons, Inc.
- 437
- 438 Miura K, Maeda K, Toki S. 1997 Method of measurement for the angle of repose of sands.  
*Soils Found.* **37**, 89–96. (doi:10.1248/cpb.37.3229)
- 439
- 440 Makse HA, Havlin S, King PR, Stanley HE. 1997 Spontaneous stratification in granular  
441 mixtures. *Nature* **386**, 379–382. (doi:10.1038/386379a0)
- 442
- 443 Scharf I, Ovadia O. 2006 Factors influencing site abandonment and site selection in a sit-  
444 and-wait predator: a review of pit-building antlion larvae. *J. Insect Behav.* **19**,197–218.
- 445
- 446 Bar-Ziv MA, Bega D, Subach A, Scharf I. 2019 Wormlions prefer both fine and deep sand but  
447 only deep sand leads to better performance. *Curr. Zool.* **65**, 1–8 (doi:10.1093/cz/zoy065)
- 448
- 449 Allen GR, Croft DB. 1985 Soil particle size and the pit morphology of the Australian ant-lions  
450 *Myrmeleon diminutus* and *M. pictifrons* (Neuroptera: myrmeleontidae). *Aust. J. Zool.* **33**,863–  
451 874.
- 452
- 453 Loiterton SJ, Magrath RD. 1996. Substrate type affects partial prey consumption  
454 by larvae of the antlion *Myrmeleon acer* (Neuroptera: myrmeleontidae). *Aust. J. Zool.* **44**,  
455 589–597.
- 456
- 457 Botz JT, Loudon C, Barger JB, Olafsen JS, Steeples DW. 2003 Effects of slope  
458 and particle size on ant locomotion: implications for choice of substrate by  
459 antlions. *J. Kansas Entomol. Soc.* **76**, 426–435.

460  
461 Farji-Brener AG. 2003 Microhabitat selection by antlion larvae, *Myrmeleon crudelis*: effect of  
462 soil particle size on pit-trap design and prey capture. *J. Insect Behav.* **16**, 783–796.  
463  
464 Barkae ED, Scharf I, Abramsky Z, Ovadia O. 2012 Jack of all trades, master  
465 of all: a positive association between habitat niche breadth and foraging performance  
466 in pit-building antlion larvae. *PLoS ONE* **7**, e6.  
467  
468 Griffiths D. 1980 The feeding biology of the antlion larvae: prey capture,  
469 handling time and utilisation. *J. Anim. Ecol.* **49**, 99–125.  
470  
471 Lucas JR. 1982 The biophysics of pit construction by antlion larvae  
472 (*Myrmeleon*, Neuroptera). *Anim. Behav.* **30**, 651–664.  
473  
474 Heinrich B, Heinrich MJE. 1984 The pit-trapping foraging strategy of the antlion, *Myrmeleon*  
475 *immaculatus* DeGeer (Neuroptera: myrmeleontidae). *Behav. Ecol. Sociobiol.* **14**, 151–160.  
476  
477 Scharf I, Gilad T, Bar-Ziv MA, Katz N, Gregorian E, Pruitt JN, Subach A. 2018. The  
478 contribution of shelter from rain to the success of pit-building predators in urban habitats.  
479 *Anim. Behav.* **142**, 139–145.  
480  
481 Humeau A, Piñeirua M, Crassous J, Casas J. 2019 Locomotion of Ants Walking up Slippery  
482 Slopes of Granular Materials, *Integ. Organismal Biol.* **1**, obz020. (doi: 10.1093/iob/obz020)  
483  
484 Gorb SN, Heepe L. 2017 *Biological fibrillar adhesives: Functional principles and biomimetic*  
485 *applications*. In da Silva L, Öchsner A, Adams R. (eds.) Handbook of adhesion technology  
486 Cham, Switzerland: Springer.  
487  
488 Büscher TH, Gorb SN. 2019 Complementary effect of attachment devices in stick insects  
489 (Phasmatodea). *J. Exp. Biol.* **2019**, jeb.209833. (doi: 10.1242/jeb.209833)  
490  
491 Gepp J, Hölzel H. 1989 *Ameisenlöwen und Ameisenjungfern – Myrmeleonidae*. Wittenberg,  
492 Germany: Ziemsen Verlag.  
493  
494 Lambert EP, Motta PJ, Lowry D. 2011 Modulation in the feeding prey capture of the antlion,  
495 *myrmeleon crudelis*. *J. Exp. Zool.* **313A**, 1-8.  
496



497 Bäumler F, Koehnsen A, Tramsen HT, Gorb SN, Büsse S. 2020 Illuminating nature's beauty:  
498 modular, scalable and low-cost LED dome illumination system using 3D-printing technology.  
499 *Sci. Rep.* **10**, 12172. (doi:10.1038/s41598-020-69075-y)

500

501 *Tschuchnigg, F., Schweiger, H., Sloan, S. W., Lyamin, A. V., & Raissakies, I.*  
502 *(2015a). Comparison of finite element limit analysis and strength reduction*  
503 *techniques. Géotechnique, 65(4), 249-257.*

504

505 Davis EH. 1968 *Theories of plasticity and failure of soil masses*, In: Lee IK (Ed.) *Soil*  
506 *mechanics: selected topics*. New York, NY: Elsevier

507

508 Bongers J, Koch M. 1981 Trichterbau des Ameisenlöwen, *Euroleon nostras* (Fourcr.). *Neth.*  
509 *J. Zool.* **31**, 2.

510

511 Ortiz M, Quigley JJ. 1991 Adaptive mesh refinement in strain localisation problems.  
512 *Comput. Methods Appl. Mech. Eng.* **90**, 781-804.

513

514 Mohr O. 1900 Welche Umstände bedingen die Elastizitätsgrenze und den Bruch eines  
515 Materials? *Z. Vereines deutscher Ing.* **44**, 1524-1530

516

517 Mitchell JK, Soga K. 2005 *Fundamentals of soil behavior*. New York, NY: Wiley & Sons.

518

519 Tschuchnigg, F., Schweiger, H., & Sloan, S. W. (2015b). Slope stability analysis by means of  
520 finite element limit analysis and finite element strength reduction techniques. Part I:  
521 Numerical studies considering non-associated plasticity. *Computers and Geotechnics, 70*, 169-  
522 177.

523

## 524 **Table legends**

525

526 **Table 3:** Parameters used in the finite-element simulations for the Mohr-Coulomb model (grey zones  
527 do not influence the strength reduction method).

528

529 **Table 4:** Change in model areas to simulate the six different case via strength reduction method.

530

## 531 **Figure legends**

532 **Figure 1:** Antlion and pitfall trap. A. Habitus of antlion larva (*Euroleon nostras*), lateral view. B-C.  
533 Sandpit used from the antlion as pitfall trap. C. Same sandpit as in B including labels. D. Sand

534 throwing behaviour of the antlion by the flick of its head. D1-4. Time series based on single frames  
535 obtained from high-speed videography: 1. Before the flick of the antlion head starts; 2. During the flick,  
536 upwards movement of the antlions head; 3. During the flick, downward movement of the antlions  
537 head; 4. After the flick of the antlion head.

538

539 **Figure 2:** Axi-symmetric mesh for the initial slope model, using 1000 (15-noded) elements. The soil  
540 (blue) is modelled using the linear elastic – perfectly plastic Mohr-Coulomb model.

541

542 **Figure 3:** Slope of a sandpit before and after sand throwing by the antlion. A. Already leveled slope  
543 (caused by the prey item, house cricket on the left side) before the sand throwing of the antlion. Red  
544 line indicates the slope angle of 25.5°, the grey line indicates the reference angle. B. Slope after the  
545 sand throwing of the antlion. Blue line indicates the new slope angle of 31°, red line of the old slope  
546 angle in transparent, the grey line indicates the reference angle. C. Box-whisker-plots of initial (before)  
547 and resulting (after) slope angles of the pit. The line represents the median, the box and whiskers the  
548 10, 25, 75 and 90 % percentiles, respectively. \*  $P \leq 0.001$ , paired t-test.

549

550 **Figure 4:** Escape experiment: house cricket over the cause of 12h in a formicarium. A-C. Change of  
551 the artificial pit geometry over the cause of 12h. A 0h. B 6h. C 12h. D. Change of the slope angle over  
552 the cause of 12h, green line after 0h, blue line after 6h and violet line after 12h. E. Change of the  
553 artificial sandpit geometry over the cause of 12h shown as schematic, green after 0h, blue after 6h  
554 and purple after 12h.

555 **Figure 5:** Results for the Cases 1 – 6 (A.-F.) with the indicated change of the reduced soil volume (in  
556 red), the changed zones for the friction angle (in blue) and the results, shown as failure surfaces with  
557 different adaptive meshes, which demonstrate the failure mechanisms.

558

## 559 **Supplement**

560

561 Supplementary Video 1: Sandslides caused by antlion

562

563 Supplementary Video 2: Sandslides caused by antlion and relocalisation of prey item

564

565 Supplementary Video 3: Slope change caused by prey item with antlion

566

567 Supplementary Video 4: Slope change caused by prey item without antlion over the cause of  
568 twelve hours (12h experiment)

569

570 Supplementary Video 5: Ant escaping a antlions pitfall trap, without active antlion